Vol. **1**, **1**. 41-61 (2000)

Revue de Mécanique Appliquée et Théorique

Buckling Analysis Based on Polycristalline Plasticity

A. Zghal
Laboratoire de Mécanique des Solides et des Structures École Supérieure des Sciences et Techniques
5 Avenue Taha Hussein 1008 Montfleury Tunis Tunisie

A. Naddari
Laboratoire de Physique et Mécanique des Matériaux, UMR CNRS 7554
Université de Metz, ISGMP Ile du Saulcy F-57045 Metz Cedex 01 France

M. Potier-Ferry
Laboratoire de Physique et Mécanique des Matériaux, UMR CNRS 7554
Université de Metz, ISGMP Ile du Saulcy F-57045 Metz Cedex 01 France

Résumé
Nous revisitons le problème délicat du choix d'une loi de comportement adaptée pour modéliser le flambage des structures à paroi mince. Les théories classiques de l'écoulement et de la déformation sont comparées avec un modèle micromécanique. Nous établissons qu'un modèle polycristallin peut expliquer pourquoi la théorie de la déformation est meilleure que la théorie de l'écoulement pour prédire le flambage plastique. On réalise cette comparaison pour un problème simple de flambage, en vue de concevoir des essais de caractérisation pour évaluer la matrice des modules tangents.

Abstract
We revisit the delicate problem of choosing an appropriate constitutive law to model buckling of thin walled structures. The classical flow and deformation theories are compared with a micromechanical model. We establish that a polycrystalline modelling is able to explain why the deformation theory is better than the flow theory to predict plastic buckling. This comparison is achieved for a simple buckling problem, with a view to design characterization tests for the evaluation of the tangent stiffness matrix.

1. INTRODUCTION

The buckling of compressed elastoplastic structures is the result of complex interactions between the geometric nonlinearity and the material nonlinearity. The determination of the critical buckling load and of the post-critical behaviour has been the object of many theoretical and numerical developments, [18] [20] [17]. This work is a contribution to the delicate problem of choosing an appropriate constitutive law to model the plastic buckling of thin walled structures. In many cases, buckling occurs beyond the elastic limit, however, at small strains, usually lower than 2 %. For this reason and for sake of simplicity, we shall limit ourselves to the small strain case.
Shanley (1947) [19] established that the buckling of a compressed beam is characterised by a bifurcation criterion and that the critical load is proportional to the tangent modulus of the material. Hill (1958) [7] generalised the principle of Shanley and developed the theory of bifurcation and

uniqueness for three dimensional elastic-plastic solids. This theory forms the basis of the present investigation. Hill introduces a quadratic functional, which, in the small strain case, can be written as follows:

$$F(\tilde{u}) = \int (L_{ijkl}\tilde{\varepsilon}_{ij}\tilde{\varepsilon}_{kl} + \sigma^0_{ij}\tilde{u}_{k,i}\tilde{u}_{k,j})dv \quad (1)$$

where σ^0_{ij} is the stress which exists in the fundamental state before bifurcation and the moduli L_{ijkl} correspond to the so called "elastic comparison solid". $\tilde{u}_k$ denotes the displacement component, dv is the volume element. Further, a comma followed by a subscript implies differentiation with respect to the appropriate coordinate and the summation convention is understood. For instance, if the constitutive law involves a smooth yield surface, these moduli are equal to the plastic tangent moduli wherever the stress is on the yield surface (whatever be the stress rate) and equal to the elastic moduli elsewhere [9] [20]. The first bifurcation point is obtained when this functional F can be zero.

It is very well known that bifurcation loads predicted by the simplest incremental theory of plasticity (J_2 flow theory; denoted as J_2F in this paper), overestimates the experimental buckling loads of plates and shells. On the contrary, the analysis based on the deformation theory of plasticity (J_2 deformation theory; denoted as J_2D), often conforms quite enough agreement with the experimental results. Let us mention that the phenomenological corner theory developed by Christoffersen and Hutchinson [2] is more satisfactory because it is an incremental constitutive law that coincides with J_2D in proportional monotonic loading.

In the analysis of structural buckling, several pragmatic methods have been proposed to overcome this basic difficulty and to be able to predict realistic buckling loads. The general idea is to use an incremental plasticity framework for the prebuckling calculations and to introduce an alternative suitable tensor **L** in subroutines for bifurcation's checks, i.e. in the buckling criterion (1).

The most common choice is a stiffness tensor **L** deduced from deformation theory. Bushnell [1] did specific correction for the shear modulus which is the most sensitive one in the buckling analysis. A cruder but simpler method proposed by Combescure [3], is to equally reduce all the components of the tensor **L** with respect to the elastic tensor $\mathbf{L}^e$.

$$\mathbf{L} = \frac{E_t}{E}\mathbf{L}^e \quad (2)$$

The latter way, that is not widely used, presented here as a lower bound or as a reference for a discussion.

It is now common to evaluate tangent stiffness tensors by polycrystalline models. In a pioneering work, Hutchinson (1970) [11] has established that all the components of the stiffness decrease when the strain increases, but they do not decrease equally as predicted by relation (2). Especially, the shear modulus decreases strongly in uniaxial loading while it is constant according to the flow theory. So the micromechanical models Are able to explain, at leas qualitatively, the difference between the experiments and the prediction of the flow theory. A similar approach will be used in this paper in order to evaluate the ability of all those methods for buckling analysis.

Nevertheless, no significant works were done on the implication of the polycrystalline plasticity in structural buckling. Furthermore, in the paper [11], the application of polycrystalline models to buckling is implicit, for only the evolution of the three dimensional stiffness tensor is analysed. In this paper, first we compute the evolution of the plane stress tensor that is the more relevant for plate and shell analysis. Then we apply the results to a specific buckling problem, i.e. the buckling of rectangular simply supported plate in uniaxial compression.

A rough design of experimental tests to evaluate the evolution of the tangent stiffness tensor can be suggested from the point of view of this analysis.
There is another reason to start again the discussion of the most appropriate law to predict structural buckling. Indeed, significant progress has been achieved since the work of Hutchinson [11], see for instance Hihi [6], Iwakuma and Nemat-Nasser [12] , Lipinski and Berveiller [13], Lipinski et al [14] and Desbordes [4]. Here, the self-consistent model by Lipinski, Naddari and Berveiller [15] will serve as a reference to evaluate the performance of the classical phenomenological laws for buckling analysis.
With respect to older works on micromechanical modelling, the most important improvement for the present discussion is the account of hardening and interaction between glide systems. The aim of this paper is therefore to revisit the problem, with account for the significant progress done in the last decade. For this reason, we did not wante first to develop a new micromechanical model even if our reference model may be discussed and improved.

2. INFLUENCE OF THE CONSTITUTIVE LAW ON THE SHAPE OF THE TANGENT STIFFNESS MATRIX

In this part we compare three models of plasticity: the classical laws J_2F and J_2D and a self-consistent method applicable to BCC metals. In the practice of structural analysis, one introduces modulus deduced from uniaxial stress-strain law easily obtained by experiment. That is why we are interested to the shape of the tangent matrix, more precisely in the evolution of the ratios of different stiffness moduli as a function of loading.
The deformation theory considers that the plastic strain ε_{ij}^{p} is only a function of the stress σ_{ij} in the actual state, without taking into account loading history. By contrast, the incremental theory expresses the plastic strain increment $d\varepsilon_{ij}^{p}$ in the actual stress state σ_{ij} as a function of the stress increment $d\sigma_{ij}$.
These models are very well known, see for instance Neale [16]. Here the chosen incremental theory corresponds to isotropic hardening, but our conclusions would not be significantly modified if we had also considered kinematic hardening.
The corner theory has not been considered in this paper because it yields the same results as the deformation theory.
In polycrystalline models, the phenomenological laws are introduced at the scale of single crystalline grains and the constitutive law is obtained by a homogeneization method. In this paper, we apply the model described in Lipinski, Naddari and Berveiller [15]. At the crystal level, it is assumed that the plastic deformation is only due to the slip of single crystals. The evolution of the critical shear stresses is governed by a classical hardening law, Hill [8]. The polycrystal is an assembly of grains with various forms (morphological textures) and various crystalline orientations (crystallographic textures). Hill's formalism is used for the transformation between quantities at local and overall scales and the macroscopic behaviour is obtained by the self-consistent method.

2.1. Analysis of phenomenological constitutive laws

We now discuss the shape of the compliance matrix in purely uniaxial traction or compression and with a plane stress state. In the case of the J_2 deformation and J_2 flow models, the relation between the stress increment and the strain increment is written as:

$$\dot{\sigma}_{ij} = L_{ijkl}\,\dot{\varepsilon}_{kl} \tag{3}$$

$$L_{ijkl} = L^{e}_{ijkl} - 2\alpha \frac{G_J}{g_J} \sigma'_{ij}\sigma'_{kl} \tag{4}$$

$$\alpha = \begin{cases} 0 & \text{in elastic loading or unloading} \\ 1 & \text{in plastic loading} \end{cases}$$

$$\sigma'_{ij} = \sigma_{ij} - \frac{1}{3}\delta_{ij}\sigma_{kk} \qquad \text{deviatoric stress}$$

$$g_J = \frac{2}{3}\bar{\sigma}^2\left(1 + \frac{h_J}{2G_J}\right)$$

with $\bar{\sigma}^2 = \frac{3}{2}\sigma'_{ij}\sigma'_{ij}$ $\qquad \frac{1}{h_J} = \frac{3}{2}\left(\frac{1}{E_t} - \frac{1}{E_J}\right)$

and $G_J = \frac{E_J}{2(1+\nu_J)}$

in J_2F case

$$\nu_J = \nu, \qquad E_J = E \tag{5}$$

in J_2D case

$$\nu_J = \nu_s, \qquad E_J = E_s \tag{6}$$

with

$$\nu_s = \frac{1}{2} + \frac{E_s}{E}\left(\nu - \frac{1}{2}\right)$$

where ν, E, E_t, E_S are respectively the elastic Poisson's ratio, Young's modulus, tangent and secant moduli. L^{e}_{ijkl} is the stiffness tensor in the J_2F case and it is the secant stiffness tensor in the J_2D case:

$$L^{e}_{ijkl} = 2G_J\left[\frac{1}{2}(\delta_{ik}\delta_{jl} + \delta_{il}\delta_{jk}) + \frac{\nu_J}{1-2\nu_J}\delta_{ij}\delta_{kl}\right]$$

These can be expanded as follows:

$$\begin{Bmatrix} \dot{\varepsilon}_{11} \\ \dot{\varepsilon}_{22} \\ \dot{\varepsilon}_{12} \end{Bmatrix} = \frac{1}{E_1} \begin{bmatrix} 1 & -\nu_{21}\frac{E_1}{E_2} & 0 \\ -\nu_{12} & \frac{E_1}{E_2} & 0 \\ 0 & 0 & \frac{E_1}{G_{12}} \end{bmatrix} \begin{Bmatrix} \dot{\sigma}_{11} \\ \dot{\sigma}_{22} \\ \dot{\sigma}_{12} \end{Bmatrix} \tag{7}$$

where $E_1=E_t$. The matrix is therefore described by three nondimensional parameters in ratio form ν_{12}, E_2/E_1 and G_{12}/E_1. Their expressions are given by:

	J_2D	J_2F
ν_{12}	$\frac{1}{2}(1-\frac{E_t}{E}+2\nu\frac{E_t}{E})$	$\frac{1}{2}(1-\frac{E_t}{E}+2\nu\frac{E_t}{E})$
$\frac{E_2}{E_1}$	$4\frac{E_s}{3E_t+E_s}$	$4\frac{E}{3E_t+E}$
$\frac{G_{12}}{E_1}$	$\frac{E}{E_t}\frac{E_s}{(3E-E_S+2\nu E_s)}$	$\frac{1}{2}\frac{E}{(1+\nu)}\frac{1}{E_t}$

Table 1: Parameters in ratio form.

In Table 1, it can be seen that the shear modulus in J_2F theory remains equal to the elastic value. This well known result is the main disadvantage of flow theories. Indeed, it seems obvious that a traction loading activates several slip systems in the polycrystal and that this induces a reduction of all stiffness moduli, and especially of the shear modulus. That is why buckling experiments on cruciform specimens are in complete disagreement with the flow theory predictions [10].
The ratio E_2/E_1 of the J_2F law is also somewhat arbitrary. For rather large deformations, the ratio E_t/E is small and the ratio E_2/E_1 takes an approximate value equal to 4 without any physical basis.
The Poisson's ratio ν_{12} is the same for the two theories and varies in quite natural way from its elastic value up to 0.5 (plastic incompressibility).
Consider for example a conventional uniaxial stress-strain power law:

$$\bar{\varepsilon} = \begin{cases} \frac{\bar{\sigma}}{E} & \text{if} \quad \bar{\sigma} < \sigma_y \\ \frac{\sigma_y}{nE}\left[(\frac{\bar{\sigma}}{\sigma_y})^n + n - 1\right] & \text{if} \quad \bar{\sigma} \geq \sigma_y \end{cases} \tag{8}$$

This stress-strain representation (figure 1.1) ensures the continuity of tangent modulus. With σ_y = 170 MPa and n = 8, the evolution of the tangent modulus and secant modulus is represented in figure 1.2. The tangent modulus decreases quickly when the deformation increases, its value is only 1/170 of its initial value for a plastic strain of 2 %. The secant modulus also decreases but more

slowly.

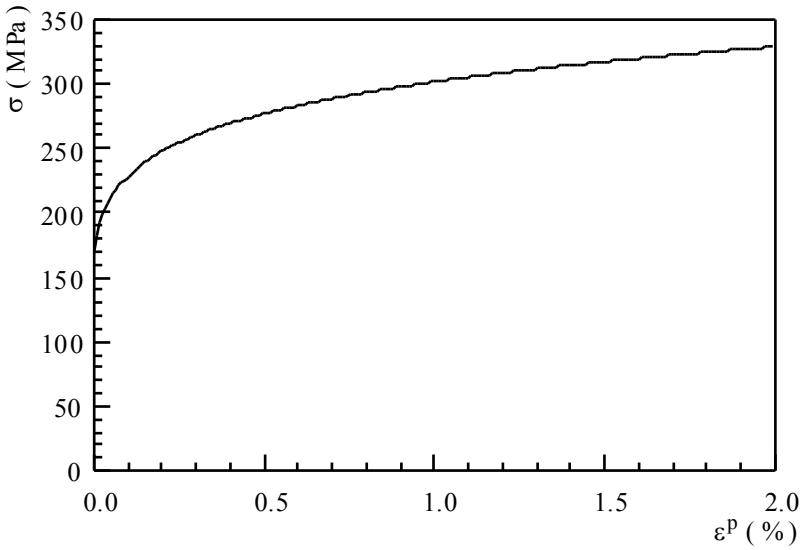

Figure 1-1: Stress strain curve for the power law (8).

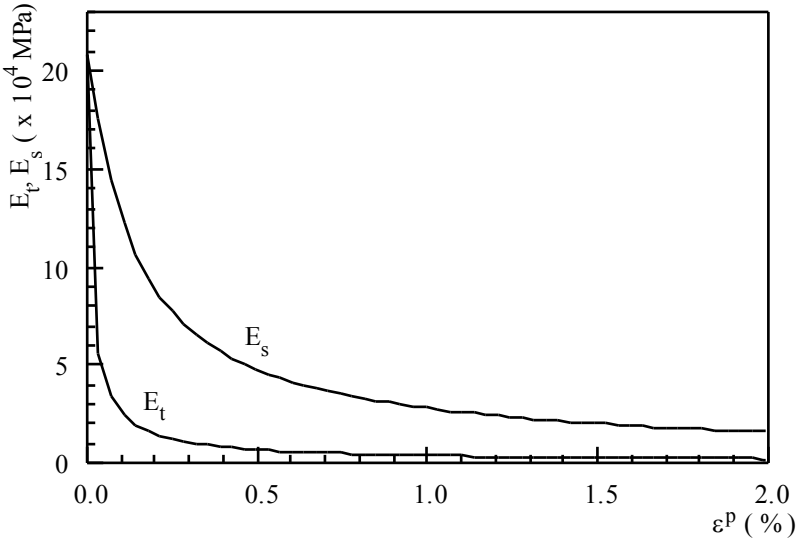

Figure 1-2: Evolution of the tangent and the secant modulus for the power law (8).

The evolutions of the three ratios ν_{12}, E_2/E_1 and G_{12}/E_1 are represented in figures 1.3, 1.4 and 1.5. The ratios E_2/E_1 and G_{12}/E_1 increase with the deformation which means that the most decreasing stiffness modulus corresponds to the applied loading.

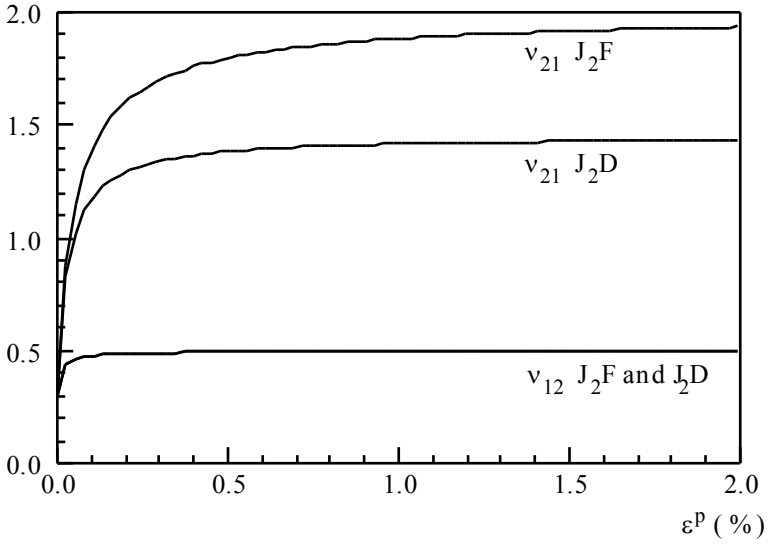

Figure 1-3: Evolution of Poisson ratios for the models J_2F et J_2D.

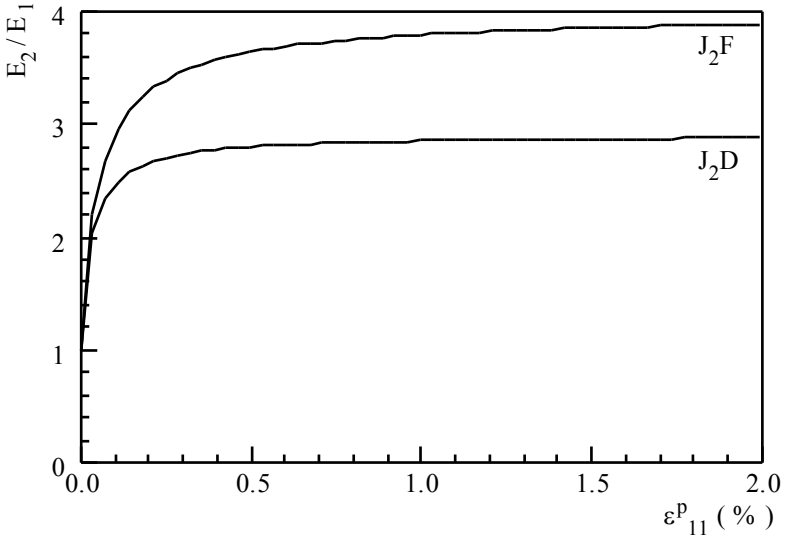

Figure 1-4: Evolution of the ratio $\frac{E_2}{E_1}$ for the models J_2F et J_2D

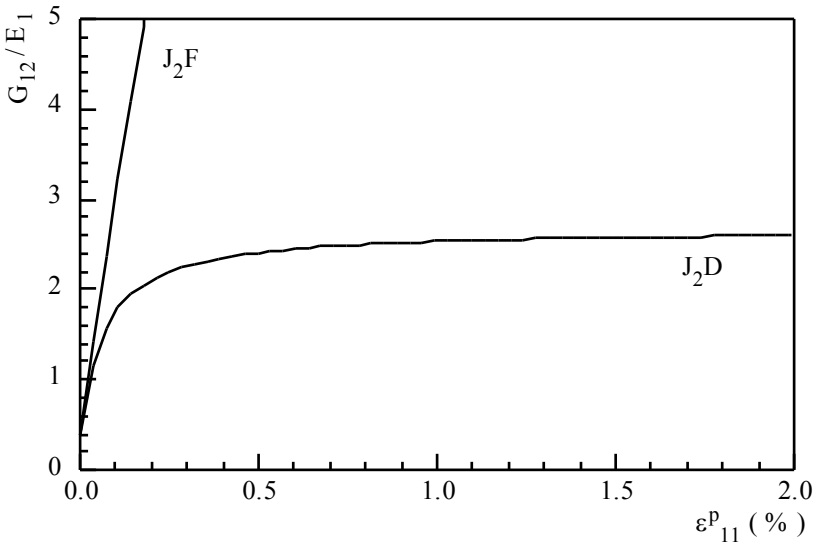

Figure 1-5: Evolution of the ratio $\frac{G_{12}}{E_1}$ for the models J_2F et J_2D.

So the "method of tangent modulus" (2) is very pessimistic by comparison with J_2F and J_2D because these ratios are assumed to be constant according to this buckling criterion. Those two models do not yield very different results for the ratio E_2/E_1. Especially, for large strains, the ratio E_2/E_1 tends to 4 for J_2F and to a lower value $4n/(3+n)$ for J_2D. Note that this limit values are not physically based and depend only on the a priori assumptions about the form of the constitutive law.

As for the ratio G_{12}/E_1, it is very large in the J_2F case, because the numerator is constant and equal to its elastic value, and the denominator is the tangent modulus, that decreases strongly. In the J_2D case, this ratio varies about as E_2/E_1, and it tends to $n/3$ for large strains, which is more realistic.

The common prediction for the Poisson's ratio ν_{12} is quite clear: it varies monotonically from its elastic value up to 0.5, which corresponds to plastic incompressibility. Because of the symmetry relation $\nu_{12} = \nu_{21} E_2/E_1$ the second Poisson's ratio has a stronger variation, that follows mainly from the evolution of the ratio E_2/E_1 that is represented in figure.1-3.

2.2 Comparison between phenomenological and polycrystalline models

In this paper, we use the recent elastoplastic polycrystalline model of [15] . In this model, the overall behaviour for the polycrystal is determined from the various physical parameters describing the structure and the state of the aggregate. The transition relations between local (microscopic) and overall (macroscopic) levels are obtained by a cinematic integral equation solved by a self-consistent scheme approximation.

The initial state of the elastic behaviour of the BCC single crystal is defined by the shear modulus of G=80 GPa and Poisson's ratio ν =0.3. We assume that the pencil glide can be described by two families of slip systems {110} <111> and {112} <110> having the same initial critical shear stress (58 MPa) in all the grains. The hardening matrix describing the interactions between the 48 glide systems, is chosen according to the experiments by Franciosi (1983). This matrix contains only two terms H_1 and H_2. H_1 corresponds to the slope in stage II of a single crystal experiment. H_1 is deduced

from latent hardening experiments. They are assumed to be constant (linear hardening) and nearly equal to G/500 and 1.1G/500 where G is the elastic shear modulus.
In order to avoid a loss of statistical informations and to describe accurately the polycrystalline edifice, the number of grains is 500. In the initial state, they possess the same spherical shape and their crystallographic orientations are chosen in a random manner to simulate an initially isotropic material.

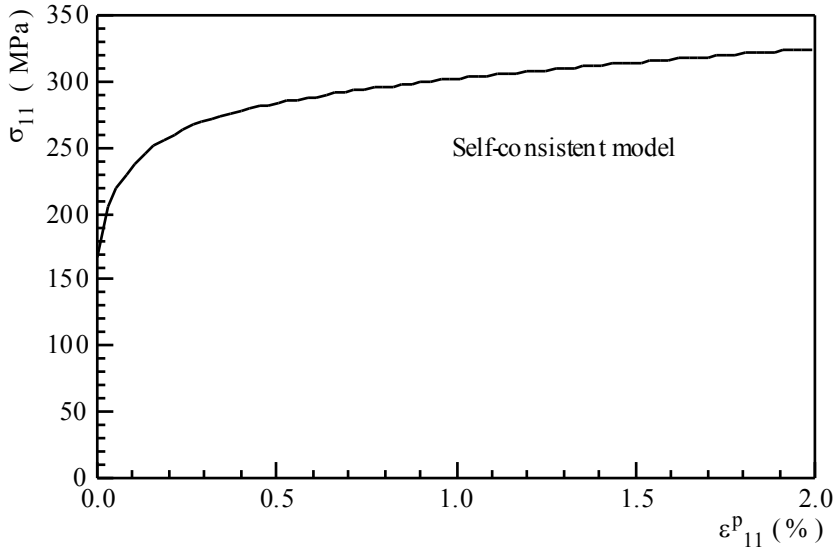

Figure 2: Stress strain curve obtained by the self-consistent model.

Figure 2 represents the stress-strain curve of $\sigma_{11} = f(\varepsilon_{11}^p)$ for uniaxial compression obtained by the self-consistent model. It has a tendency of having a parabolic regime until towards 1 % of plastic strain, and it becomes more or less linear after, which follows from the hypothesis of a constant monocrystalline hardening.
Figure 3 describes the evolution of the tangent modulus $E_t = d\sigma_{11}/d\varepsilon_{11}$ and of the secant modulus $E_s = d\sigma_{11}/d\varepsilon_{11}$ as a function of the macroscopic strain ε_{11}^p. One notes a fast decreasing of E_t, then an asymptotic tendency. The secant modulus has a similar behaviour but less marked.

In what follows, we compare the evolution of the shape of the tangent stiffness matrix for the two phenomenological laws and for the self-consistent models. Nevertheless, the phenomenological models require the knowledge of an uniaxial stress-strain law especially of the tangent modulus or of the secant modulus. In order to have a consistent comparison, we use the tangent modulus and the secant modulus predicted from the self-consistent model (figure 3), which we have reported in the expressions in table 1. So we compare the ratios predicted by the three models (J_2F, J_2D and SC). The modification of the uniaxial stress-strain law will lead to slight changes with respect to the previous results in figure 1.

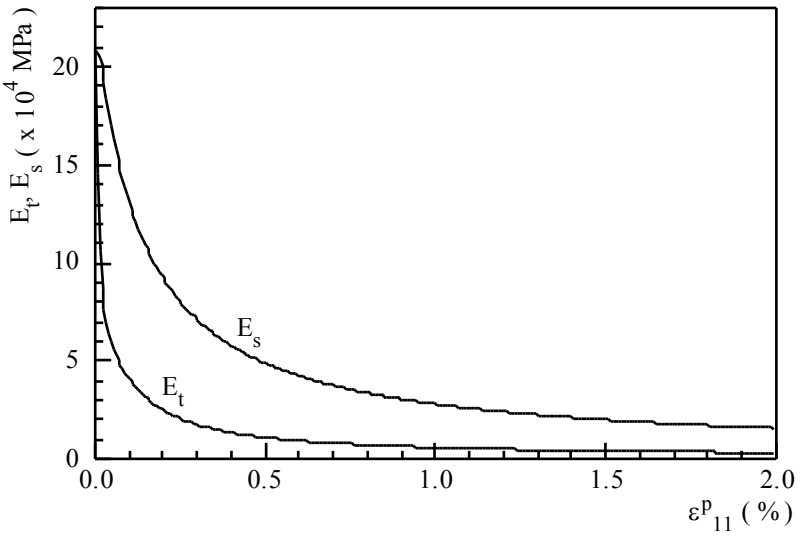

Figure 3: Evolution of the tangent and secant modulus deduced from the self-consistent model.

In figure 4, the ratio E_2/E_1 is represented as a function of the plastic strain. For the self-consistent model, it reaches a maximum of about 1.7 at a very small strain, next it decreases and tends to a value close to unity. So with regards to this ratio, the method of the tangent modulus seems in a rather good agreement with self-consistent predictions.

As for the phenomenological models, they give similar results as those of figure.1-3. They are not identical because of the slight change we have just introduced in the uniaxial law. This ratio is nearly constant for plastic strains larger than 0.5 %, the asymptotic values being about 4, 2.2, 1 for respectively the J_2F, J_2D and SC model.

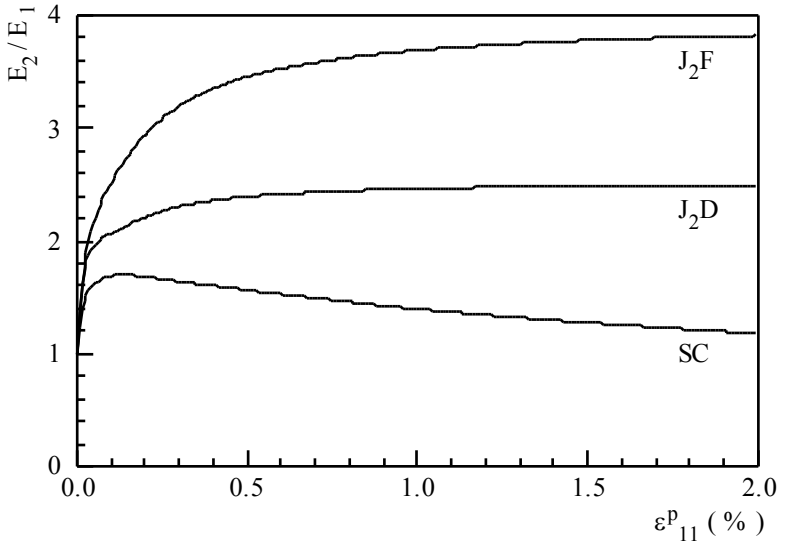

Figure 4: Evolution of the ratio E_2/E_1 for the two phenomenological models J_2F and J_2D and for the self-consistent model SC.

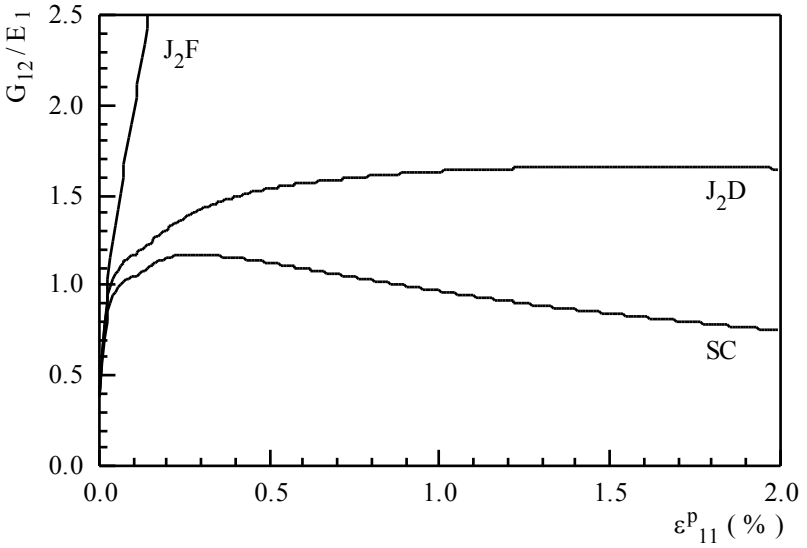

Figure 5: Evolution of the ratio G_{12}/E_1 for the two phenomenological models J_2F and J_2D and for the self-consistent model SC.

Figure 5 shows the evolution of the most sensitive parameter, i.e. the shear modulus. As discussed previously, the ratio G_{12}/E_1 becomes rapidly very large and unrealistic for J_2F. The results concerning J_2D and SC are in a qualitatively good agreement. First the ratios G_{12}/E_1 increase significantly from their initial value (0.38) and become larger than 1 for a plastic strain of 0.1 %. Hence, the method of the tangent modulus is a bit pessimistic for the shear behaviour. Beyond 0.5 %, an increasing discrepancy has been observed between J_2D and SC, the value of the ratios for ε^p = 2 % being respectively 1.5 and 0.75. Nevertheless, the present results from the self-consistent model are remarkably close to those of deformation theory.

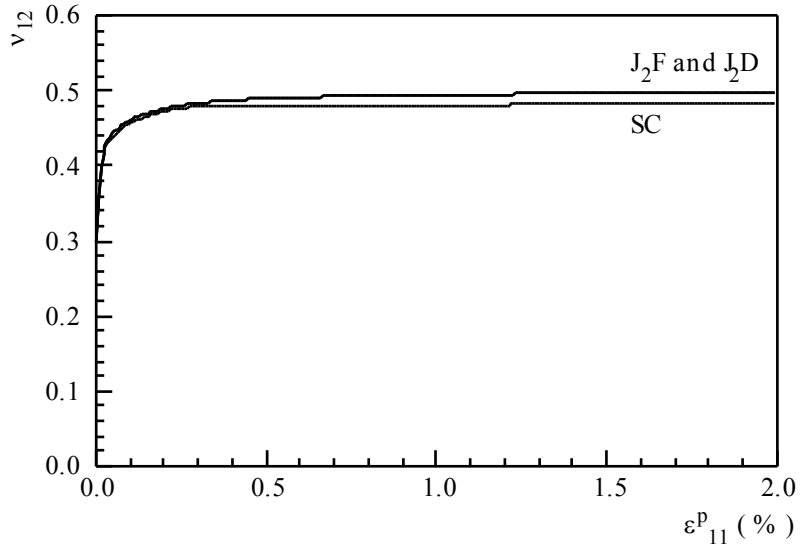

Figure 6: Evolution of the Poisson's ratio for the two phenomenological models J_2F and J_2D and for the self-consistent model SC.

The Poisson's ratio ν_{12} seems almost independent of the model as presented in figure. 6. Beyond a plastic strain of 0.5 %, this ratio is almost constant and near to incompressibility, for all three models. As discussed before, the second Poisson's ratio ν_{21} has a different behaviour, that is mostly related to that of the ratio E_2/E_1.

All these results confirm that the flow model yields inconsistent predictions, that are in a complete disagreement with other theories, as well as with experiments, (see for instance [9]). First of all, the polycrystalline model yields ratios E_2/E_1 and G_{12}/E_1 always greater than their initial value. Therefore the predictions obtained by the tangent modulus method should be conservative, which has been established by many applications [3]. Second, the two phenomenological models give ratios E_2/E_1 and G_{12}/E_1 that are always greater than the polycrystalline one. The deformations theory yields better results and there is a good qualitative agreement between J_2D and the self-consistent model. Because the third ratio ν_{12} is not sensitive to the model, further comparisons in uniaxial loading should be concentrated on the evolution of E_2/E_1 and G_{12}/E_1.

Let us remark that the ratio G_{12}/E_1 predicted by the deformation theory at $\varepsilon^p = 2\%$ is about double of the value predicted by the polycrystalline model, which could be considered as a large discrepancy. Nevertheless, in the famous tests on cruciform column, the buckling load is very sensitive to the geometrical imperfections [10]. Further, slight change in the loading direction induces an increase of the shear modulus obtained by a polycrystalline model [11]. Last, we shall see that the discrepancy in terms of tangent moduli does not involve the same gap in terms of the critical load. That is why we think that the result presented in Fig. 5 confirms the ability of the deformation theory to simulate the buckling strength of complex structures in proportional loading.

3. INFLUENCE OF THE CONSTITUTIVE LAW ON A SIMPLE BUCKLING TEST.

In the previous part, we have established that, for some plane stress and symmetry assumptions, the tangent constitutive behaviour depends mainly on two ratios E_2/E_1 and G_{12}/E_1. The final goal is to design experimental tests, to evaluate the evolution of these two ratios and to discuss the performance of constitutive models for buckling analysis. We have chosen here buckling of thin rectangular simply supported plates in uniaxial compression because:

- it is rather easy to be carried out.
- it is not very sensitive to imperfections.
- the mode shape does not depend strongly on the material properties and it is known analytically.

3.1 Buckling analysis

We consider a simply supported rectangular plate of length a, width b and thickness h under uniaxial compression. For convenience, the plate is referred to coordinate system x-y and the compressive load P_X acts on the two sides parallel to y axis. The plate remains flat and the response curve is unique up to the critical load or the bifurcation buckling load. Beyond the buckling load, there are at least two possible response curves. One of these curves is the continuation of the prebuckling curve (first part of the equilibrium path) and it is called fundamental solution. The other ones are called bifurcated or

postbuckling paths.

In the present paper, we only study the prebuckling stage and the bifurcation load. In this respect we work with modal quantities that are linearized differences between the fundamental and the bifurcated solution. Such modal quantities will be designated by ( )*. We consider Kirchhoff plates without shear deformation. Within this framework, the bending incremental law yields incremental bending moments as function of the second derivatives of the out-of plane displacement w*(x,y):

$$\begin{aligned} M_x^* &= -\frac{h^3}{12}\left[\hat{L}_{1111} w^*_{,xx} + \hat{L}_{1122} w^*_{,yy}\right] \\ M_y^* &= -\frac{h^3}{12}\left[\hat{L}_{2211} w^*_{,xx} + \hat{L}_{2222} w^*_{,yy}\right] \\ M_{xy}^* &= -2\frac{h^3}{12}\hat{L}_{1212} w^*_{,xy} \end{aligned} \tag{9}$$

where $\hat{L}_{ijkl}$ are the plane stress moduli that are deduced from the three dimensional moduli by:

$$\hat{L}_{ijkl} = L_{ijkl} - \frac{L_{ij33} L_{33kl}}{L_{3333}} \tag{10}$$

Buckling load is described by the differential equation:

$$\frac{h^3}{12}\left[\hat{L}_{1111} w^*_{,xxxx} + 2(\hat{L}_{1122} + 2\hat{L}_{1212}) w^*_{,xxyy} + \hat{L}_{2222} w^*_{,yyyy}\right] = \sigma_x^0 h w^*_{,xx} \tag{11}$$

where σ_x^0 is the applied compressive stress. We assume simply supported boundary conditions, so that the problem has closed form solutions:

$$w^* = w_0^* \sin\left(\frac{m\pi x}{a}\right)\sin\left(\frac{\pi y}{b}\right) \tag{12}$$

$$\sigma_{cr} = \frac{h^2}{12b^2}\pi^2 E_1 K_c \tag{13}$$

where

$$E_1 K_c = \hat{L}_{1111} m^2 \left(\frac{b}{a}\right)^2 + 2(\hat{L}_{1122} + 2\hat{L}_{1212}) + \hat{L}_{2222}\left(\frac{a}{b}\right)^2 \frac{1}{m^2} \tag{14}$$

In formulas (13) and (14), the critical stress has been split into three factors, first the uniaxial tangent modulus, second the geometrical ratio h/b, and third a non-dimensional number K_c, that we are trying to establish. The discussion will be focused on this factor K_c which can be rewritten in the following form:

$$K_c = \frac{1}{1-\nu_{12}\nu_{21}}\left(\frac{mb}{a}\right)^2 + 2\frac{\nu_{21}}{1-\nu_{12}\nu_{21}} + 4\frac{G_{12}}{E_1} + \frac{E_2}{E_1}\frac{1}{1-\nu_{12}\nu_{21}}\left(\frac{a}{mb}\right)^2 \tag{15}$$

This number depends principally on the three constitutive ratios $\nu_{12}, G_{12}/E_1$ and E_2/E_1. It is also a function of the geometry of the plate and of the wavenumber m, via the quantity mb/a. The critical wavenumber m is the one which minimizes the function $f(mb/a)$ in (15). When a/b is sufficiently large, the minimum is relatively insensitive to the aspect ratio a/b. When the plate is sufficiently short $(b/a \le 1)$, the minimizing wavenumber is m=1. In the latter case, the minimum depends strongly on the aspect ratio. For instance for a square plate, the expressions of K_c with the phenomenological laws are given by:

In J_2F

$$E_t K_c = E\left[\frac{2}{1+\nu} + \frac{9+\frac{E_t}{E}(8\nu-1)}{(5-4\nu)-\frac{E_t}{E}(1-2\nu)^2}\right] \tag{16}$$

In J_2D

$$E_t K_c = E_s\left[\frac{4}{3-\frac{E_s}{E}(1-2\nu)} + \frac{9+3\frac{E_t}{E_s}-4\frac{E_t}{E}(1-2\nu)}{3+2\frac{E_s}{E}(1-2\nu)-\frac{E_t E_s}{E^2}(1-2\nu)^2}\right] \tag{17}$$

One sees, that, with J_2F and for rather large deformations (E_t/E small), the quantity $E_t K_c$ is almost constant and not too different from its elastic value, which has no chance to be in accordance with experiments. On the contrary, with the deformation theory, that quantity varies more or less as the secant modulus and the plasticity has a stronger influence on the critical load, as expected.

3.2 Influence of the constitutive law

In figure 7, the evolution of the ratio K_c versus the plastic strain is presented for the case of a short plate $(a/b = 0.5)$. Roughly, this number varies as the shear ratio G_{12}/E_1, in figure 5: there is a quantitative agreement between the deformation theory and the polycrystalline model, and the flow theory leads to unrealistic results.

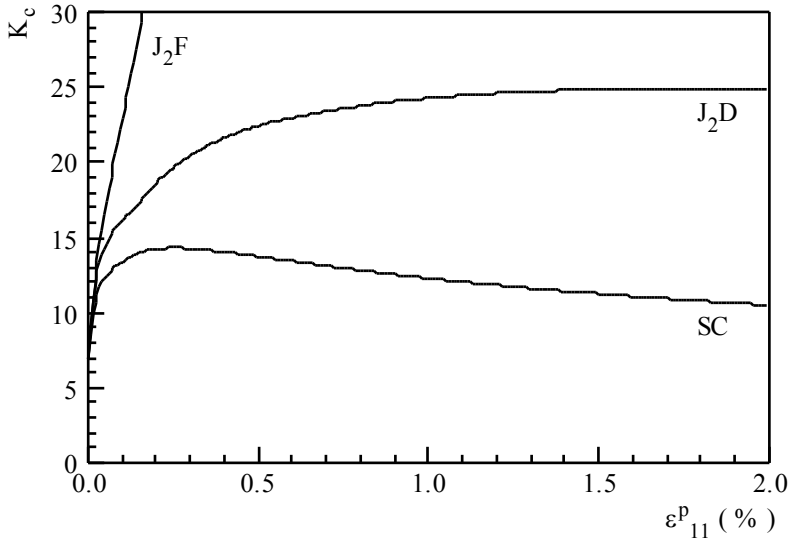

Fig.ure 7: K_c versus plastic strain for $a/b = 0.5$ for the two phenomenological models J_2F and J_2D and for the self-consistent model SC.

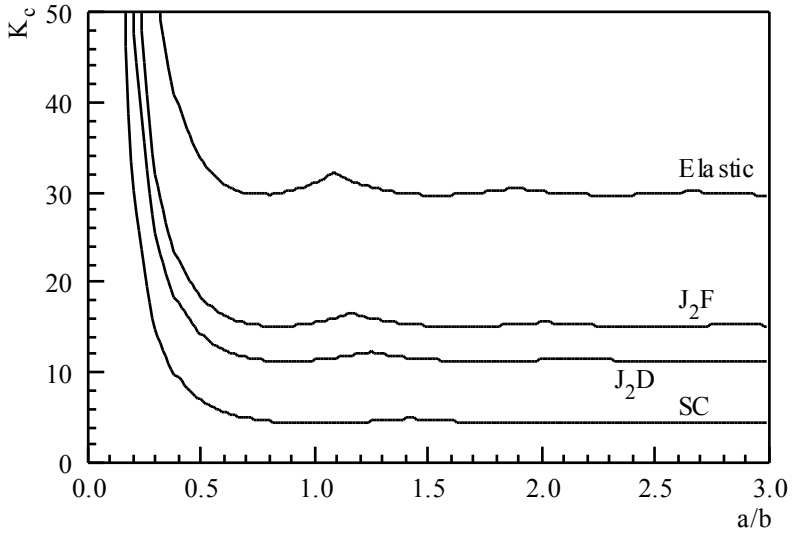

Figure 8-a: K_C versus aspect ratio a/b in the elastic case, for the tow phenomenological models and for the self-consistent model when the applied plastic strain is 0.2%.

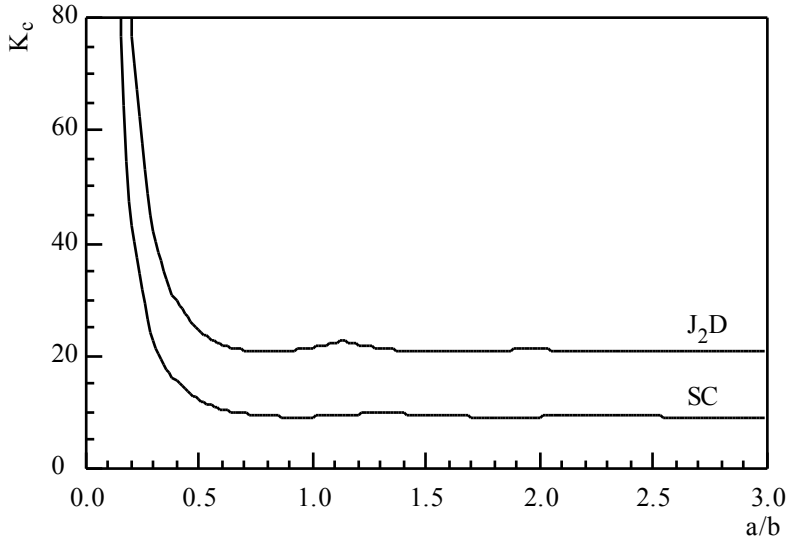

Figure 8-b: K_c versus aspect ratio a/b for the deformation theory and for the self-consistent model when the applied plastic strain is 1%.

In figure 8, the factor K_C is reported as a function of the aspect ratio, for the various models and for two plastic strain levels (0.2 % in Figure 8-a, 1 % in figure 8.b). There is a difference between deformation theory and self-consistent model but this difference remains about constant. On the contrary, the predictions of the flow theory are of the same order as with the two other models at the beginning of the plastification, but they increase rapidly with the strain: for instance at a plastic strain of 1%, K_c is larger than 140 with J_2F while it is about 20 and 10 respectively with J_2D and the polycrystalline model.

The critical stress can be deduced from the relations (13) and (14). Indeed, one can plot the quantity E_tK_c as a function of the applied stress, as in Figure 9. The critical stress is got by intersecting the curves (σ_{11}, K_cE_t) with straight lines, whose slope is a function of the ratio h/b, see formulas (13) (14). Remark that the difference between the deformation theory and polycrystalline model is not as important in terms of critical stress as in terms of the ratios G_{12}/E_1 or E_2/E_1. Indeed, by formula (13), both the increase of the load and the decrease of the tangent modulus induce plastic buckling. Therefore the strong decrease of the tangent modulus reduces the sensitivity of the buckling load with respect to the evolution of the moduli.

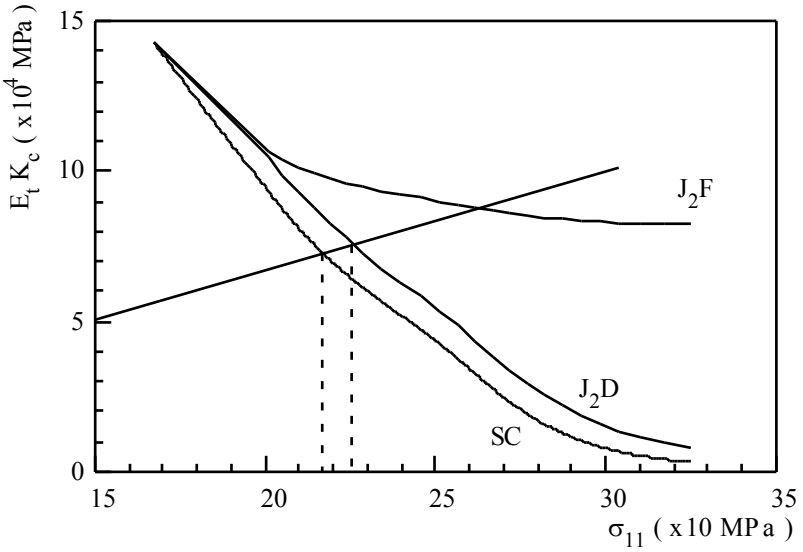

Figure 9: E_tK_c versus stress σ_{11} with an aspect ratio $\frac{a}{b}=0.5$.

3.3 Proposition of a characterization test

In this part, we try to discuss what tests are relevant to characterize the evolution of the E_1, E_2, G_{12} and ν_{12} as a function of the strain or the stress. With a simple tensile test, one can determine $E_1(\sigma)$ and $\nu_{12}(\sigma)$ but $E_2(\sigma)$ and $G_{12}(\sigma)$ are not accessible. In this respect, we could do tests with a change in the loading path, for example traction followed by shear, but at such small strains, the results will not be reliable. The idea to be drawn from this study is to suggest buckling tests, i.e. tests with a change in loading path which appears spontaneously.

In this discussion, we will try to find which possible buckling tests allow to give the evaluation of the moduli G_{12} and E_2, on the base of the buckling analysis presented here.By the formula of K_c, we can have a measure information on the shear and the transverse moduli by obtaining experimentally the critical load. Because there are two scalar quantities G_{12} and E_2 to be measured, the problem is to find at least two different tests, i.e. two different aspect ratio, such that it is possible to distinguish the contribution of each modulus G_{12} and E_2 to the buckling loads. In this respect, let us examine the contribution of the four terms on the factor Kc. Only the third term $4G_{12}/E_1$ involves the shear modulus. The three other terms involve only the transverse modulus, directly or via the second Poisson's ratio ν_{21}. In what follows we will discuss two cases: the square plate and a shorter plates ($a/b=0.5$ or lower). In figures 10 and 11, we have plotted separately the contributions of the four terms of the factor K_c. In the case of a short plate ($a/b=0.5$, figure 10), the influence of the shear modulus is rather weak because the third term is generally less than 25% of the value of the factor K_c within the deformation theory and within the polycrystalline model. Hence an experiment on a short plate would yield an indirect measurement of the transverse modulus. Furthermore, formula (15) shows that for very short plates, the factor K_c depends only on the first term, therefore on $\nu_{21}=\nu_{12}E_2/E_1$. This underlines the interest of testing very short plates. The maximal influence of the shear modulus is obtained for square or larger plates. Nevertheless, the third term is about 40% according to polycrystalline model and only 30% for the deformation theory (see figure 11). It is sufficient to get rough information on the shear modulus, but perhaps not to get an accurate

characterization. A more relevant shear modulus characterization would be obtained with alternative boundary conditions or with cruciform specimens. Of course, the achievement of such tests requires a much finer design and especially their practical implementation which is not the object of this paper.

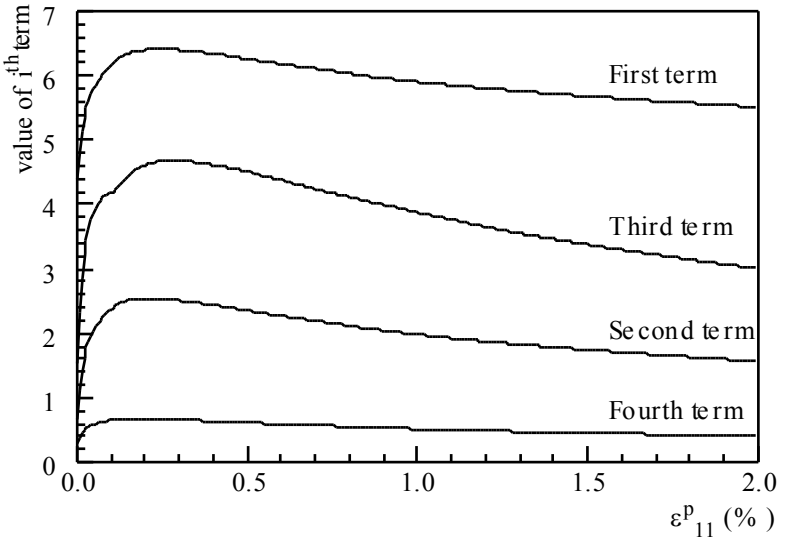

Figure 10-a: The four terms of K_c versus plastic strain according to self-consistent model SC and with an aspect ratio $a/b = 0.5$.

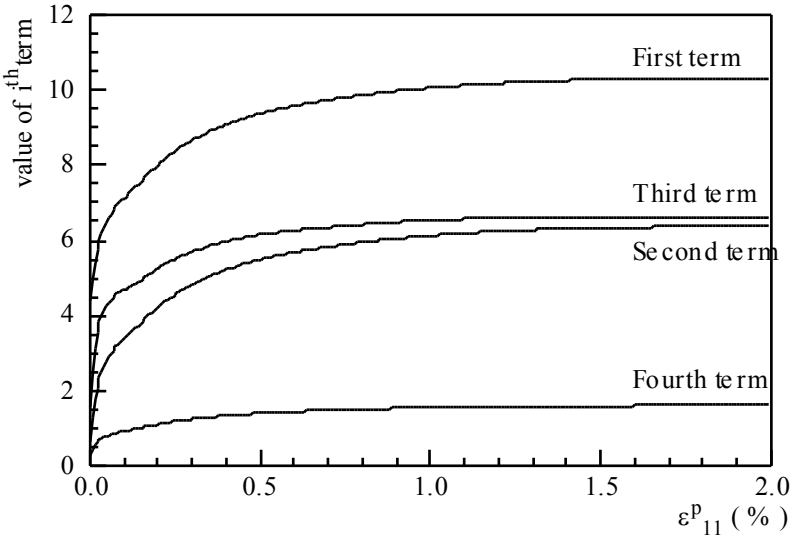

Figure 10-b: The four terms of K_c versus plastic strain according to J_2D theory and with an aspect ratio $\frac{a}{b} = 0.5$

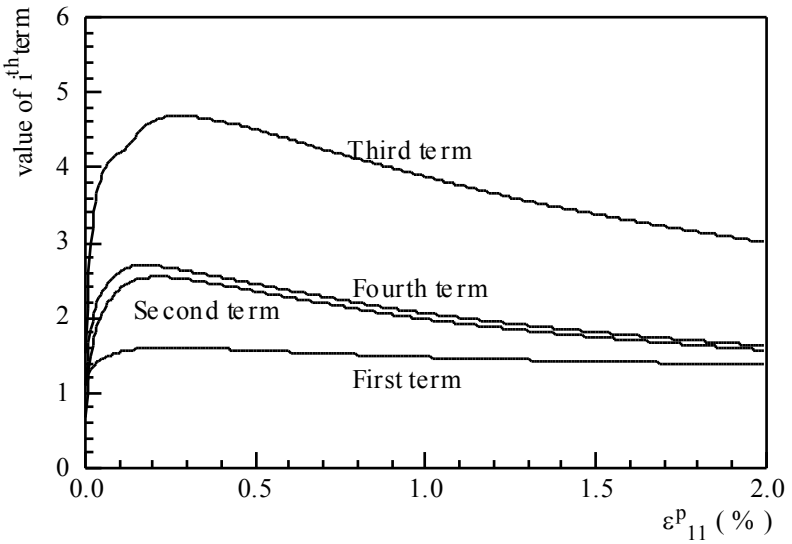

Figure 11-a: The four terms of K_c versus plastic strain according to self-consistent model SC and with an aspect ratio $\frac{a}{b}=1$.

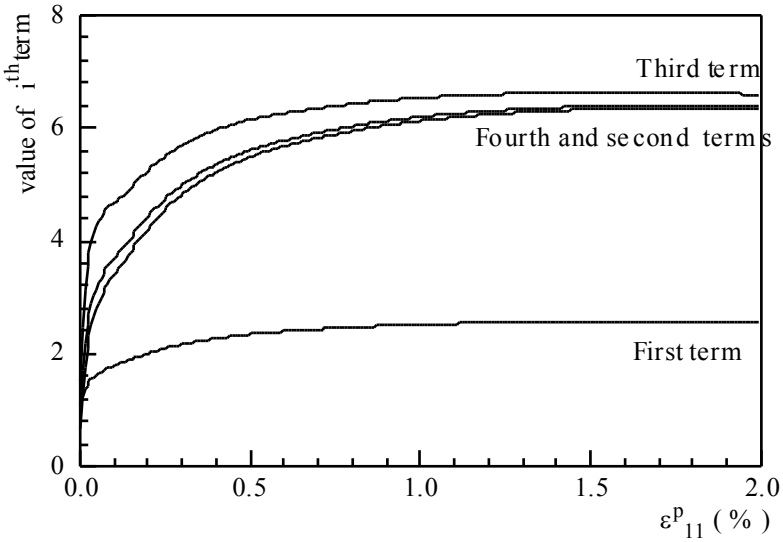

Figure 11-b: The four terms of K_c versus plastic strain according to J_2D theory and with an aspect ratio $a/b=1$.

4. CONCLUSION

In this paper, we have established that the micromechanical modelling of polycrystalline metals is sufficient to explain why the deformation theory is better than the usual flow theories to model the buckling of structures. A crucial, but not unique, feature is the evolution of the tangent shear modulus in pure compression. Indeed, it is constant within flow theory while it decreases strongly within deformation theory. The polycrystalline models lead to similar results as deformation theory because the initial crystallographic and morphological texture and the progressive evolution of the internal state of the polycrystal reduces the tangent stiffness matrix and especially the shear stiffness.

The discussion has been focused on the evolution of three ratios ν_{12}, E_2/E_1 and G_{12}/E_1 and rather strong differences between the models have been observed, at least for the two last ratios. Despite these apparent discrepancies in terms of constitutive ratios, the deformation theory and the polycrystalline model are remarkably close in terms of buckling stress. Furthermore, the present theoretical results are limited by our linearized buckling assumption, that neglects macroscopic imperfections, and the stiffening due to slight changes in macroscopic loading path, (cf. Figure 6 in [11]).

In the last part, we have discussed the influence of the constitutive modelling on a simple buckling test, with a view to design characterization tests for the evaluation of the tangent stiffness matrix. Tests on short plates will be of interest to measure the transverse tangent modulus and, perhaps, square plate tests to measure the shear modulus. Nevertheless, better measurement of the shear modulus would be obtained with specimen like the famous cruciform column.

Acknowledgement: The authors thank Marcel Berveiller and Paul Lipinski for helpful discussions.

REFERENCES

1. Bushnell D., Bifurcation buckling of shells of revolution including large deflections, plasticity and creep., Int. J. Solids Structures Vol. 10. pp. 1289-1305, (1974).
2. Christoffersen J. and Hutchinson J. W., A class of phenomenological corner theories of plasticity, J. Mech. Phys. Solids, Vol. 27. pp. 465-487, (1979).
3. Combescure A., Etude de la stabilité non linéaire géométrique et non linéaire matériau des coques minces, Habilitation à diriger des recherches, INSA de Lyon, (1995).
4. Desbordes O., editor Materiaux, Mécanique, Modélisation. Revue Européenne des Eléments Finis Vol. 3, pp. 491-595, (1994).
5. Franciosi P., Glide mechanisms in BCC crystals, Acta Metall, Vol. 31, pp. 1331-1341, (1983).
6. Hihi A., Nouvelle formulation et mise en oeuvre d'un modèle self-consistent pour l'analyse de l'écoulement anisotrope et des textures de déformation de polycristaux métalliques, Thèse d'état, Université Paris XIII, (1982).
7. Hill R., A general theory of uniqueness and stability in elastic-plastic solids, J. Mech. Phys. Solids Vol. 6, pp. 236-249, (1958).
8. Hill R., Continuum micromechanics of elastoplastic polycristals, J. Mech. Phys. Solids, Vol. 13, pp. 89-101, (1965).
9. Hutchinson J. W., Plastic buckling, Adv. Applied Mechanics Vol. 14, pp. 67-144, (1974).
10. Hutchinson J. W. and Budiansky B., Analytical and numerical study of the effects of initial imperfections on the inelastic buckling of cruciform column. Buckling of structures, (ed. B. Budiansky) Springer, Berlin, pp. 98-105, (1976).
11. Hutchinson, J. W., Elastic-plastic behaviour of polycrystalline metals and composites, Proc. Roy. Soc..Lond. A 319. pp. 247.-272, (1970).
12. Iwakuma T. and Nemat-Nasser S., Finite elastic-plastic deformation of poycristalline metals, Proc.

Roy. Soc. Lond. A304. pp. 87-119, (1984).
13. Lipinski P. and Berveiller M., Elastoplasticity of microinhomogeneous metals at large strains, .Int. J. Plast. 5, pp. 149-172, (1989).
14. Lipinski P., Krier J. and Berveiller M., Elastoplasticité des métaux en grandes déformations: comportement global et évolution de la structure interne, Rev. Phys. Appl. 25. pp. 149-172, (1990).
15. Lipinski P., Naddari A. and Berveiller M., Recent results concerning the modelling of polycrystalline plasticity at large strains, Int. J. Solids Structures, Vol. 29, pp. 1873-1881, (1992).
16. Neale K. W., Phenomenological constitutive laws in finite plasticity, SM Archives Vol. 6, pp. 79-128, (1981).
17. Nguyen Q. S., Editor, Bifurcation and stability of dissipative systems, CISM collection, Springer, Vienna, (1993).
18. Sewell M. J., A survey of plastic buckling in stability, (ed H. Leipholz) Univ. of Waterloo Press. pp. 85-197, (1972).
19. Shanley F. R., Inelastic column theory, J. Aeronaut. Sci. Vol. 14, pp. 261-267, (1947).
20. Tvergaard V., Effect of plasticity on postbuckling behaviour, Lectures Notes in physics 288. J. Arbocz, M. Potier-Ferry, J. Singer and V. Tvergaard, buckling and postbuckling. Springer-Verlag. Heidelberg, pp. 143-180, (1987).